Electron and proton acceleration at supernova remnant shocks

Christoph Pfrommer[1]

in collaboration with

PhD students: K. Ehlert,[1] L. Jlassi,[1] **R. Lemmerz,**[1]
J. Whittingham,[1] M. Weber,[1] **G. Winner**[1]
T. Berlok,[1] V. Bresci,[1] P. Girichidis,[2] **M. Pais,**[3] R. Pakmor,[4] L. Perrone,[1]
M. Shalaby,[1] M. Sparre,[5,1] **T. Thomas,**[1] M. Werhahn[1]

[1]AIP Potsdam, [2]U of Heidelberg, [3]Hebrew U, [4]MPA Garching, [5]U of Potsdam

The Variable Multi-Messenger Sky, Cracow, Nov 2022

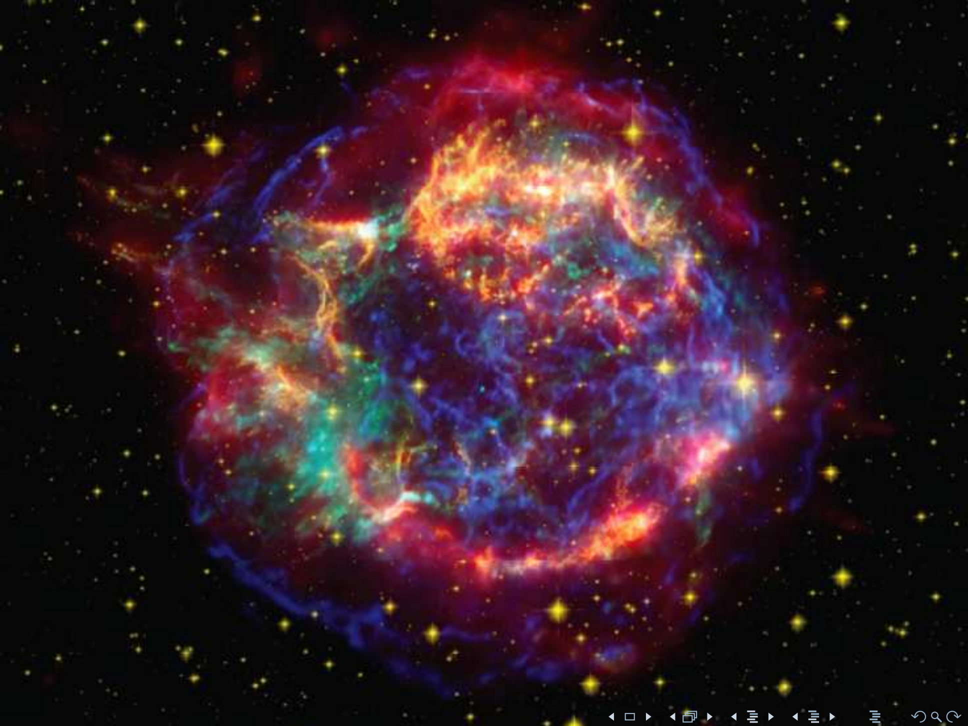

Particle acceleration: an extreme multi-scale problem

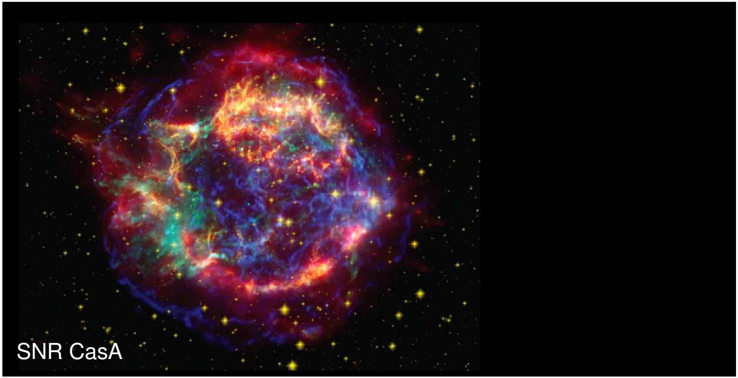

supernova remnant:

$d_{\mathrm{SNR}} \sim 6\ \mathrm{pc} \sim 2 \times 10^{19}\ \mathrm{cm}$,

Particle acceleration: an extreme multi-scale problem

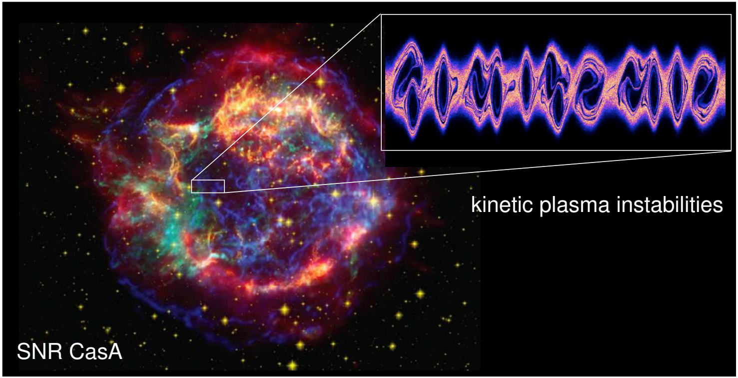

supernova remnant:

$$d_{\mathrm{SNR}} \sim 6\ \mathrm{pc} \sim 2 \times 10^{19}\ \mathrm{cm},$$

plasma skin depth:

$$\lambda_{\mathrm{i}} = \frac{c}{\omega_{\mathrm{i}}} \sim 2 \times 10^{7} \left(\frac{n}{1\ \mathrm{cm}^{-3}}\right)^{-1/2} \mathrm{cm}$$

Particle acceleration: an extreme multi-scale problem

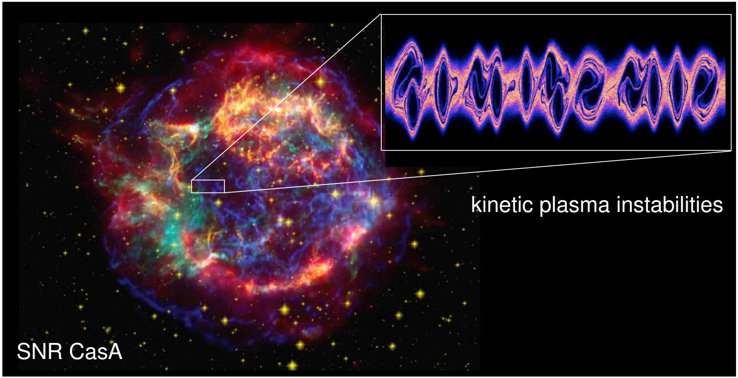

supernova remnant:

$$d_{\mathrm{SNR}} \sim 6\ \mathrm{pc} \sim 2\times10^{19}\ \mathrm{cm},$$

plasma skin depth:

$$\lambda_{\mathrm{i}} = \frac{c}{\omega_{\mathrm{i}}} \sim 2\times10^{7}\ \left(\frac{n}{1\ \mathrm{cm}^{-3}}\right)^{-1/2}\ \mathrm{cm}$$

$\Rightarrow$ need to develop a **multi-scale approach: PIC and MHD models!**

Outline

Interactions of cosmic rays (CRs) and magnetic fields

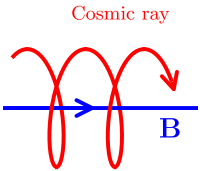

sketch: Jacob & CP

Interactions of cosmic rays (CRs) and magnetic fields

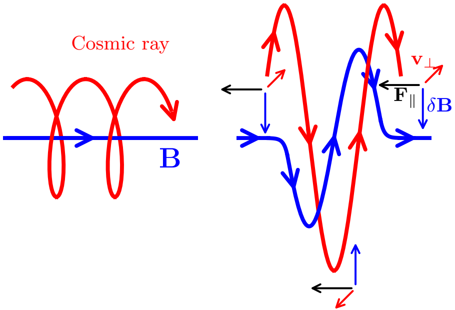

sketch: Jacob & CP

- **gyro resonance:** $\omega - k_{||} v_{||} = n\Omega$

  Doppler-shifted MHD frequency is a multiple of the CR gyrofrequency

Interactions of cosmic rays (CRs) and magnetic fields

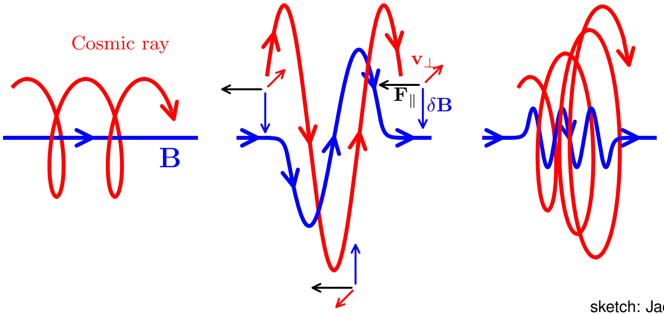

sketch: Jacob & CP

- **gyro resonance:** $\omega - k_{||} v_{||} = n\Omega$
  Doppler-shifted MHD frequency is a multiple of the CR gyrofrequency
- CRs scatter on magnetic fields $\rightarrow$ isotropization of CR momenta

Cosmic ray scattering with background plasma

- extrinsic confinement: scattering off of turbulent plasma modes injected on the driving scale and cascaded to smaller scales
  $\Rightarrow$ important for confinement of TeV CRs

Cosmic ray scattering with background plasma

- extrinsic confinement: scattering off of turbulent plasma modes injected on the driving scale and cascaded to smaller scales
  $\Rightarrow$ important for confinement of TeV CRs
- intrinsic confinement: CRs drive unstable plasma wave modes (e.g., Alfvén waves), and then scatter off of them
  $\Rightarrow$ most important mechanism for GeV CR confinement

Cosmic ray scattering with background plasma

- extrinsic confinement: scattering off of turbulent plasma modes injected on the driving scale and cascaded to smaller scales
  $\Rightarrow$ important for confinement of TeV CRs
- intrinsic confinement: CRs drive unstable plasma wave modes (e.g., Alfvén waves), and then scatter off of them
  $\Rightarrow$ most important mechanism for GeV CR confinement
- dispersion relation ($\Omega_{\mathrm{e},0} = -m_\mathrm{i}/m_\mathrm{e} \times \Omega_{\mathrm{i},0}$, $\alpha = n_\mathrm{cr}/n_\mathrm{i}$): gyrotropic CR ion + electron beam propagates in background plasma

$$\frac{k^2c^2}{\omega^2} - 1 = \frac{\omega_\mathrm{i}^2}{\omega\left(-\omega \pm \Omega_{\mathrm{i},0}\right)} + \frac{\omega_\mathrm{e}^2}{\omega\left(-\omega \pm \Omega_{\mathrm{e},0}\right)} \quad \Leftarrow \text{ background}$$

$$\text{CRe} \Rightarrow \quad + \frac{\alpha\omega_\mathrm{e}^2}{\gamma_\mathrm{e}\omega^2}\left\{\frac{\omega - kv_\mathrm{dr}}{kv_\mathrm{dr} - \omega \mp \Omega_{\mathrm{e},0}/\gamma_\mathrm{e}}\right\}$$

$$\text{CRi} \Rightarrow \quad + \frac{\alpha\omega_\mathrm{i}^2}{\gamma_\mathrm{i}\omega^2}\left\{\frac{\omega - kv_\mathrm{dr}}{kv_\mathrm{dr} - \omega \pm \Omega_\mathrm{i}} - \frac{v_\perp^2\left(k^2c^2 - \omega^2\right)/c^2}{2\left(kv_\mathrm{dr} - \omega \pm \Omega_\mathrm{i}\right)^2}\right\}$$

AIP

CR driven instabilities – growth rates

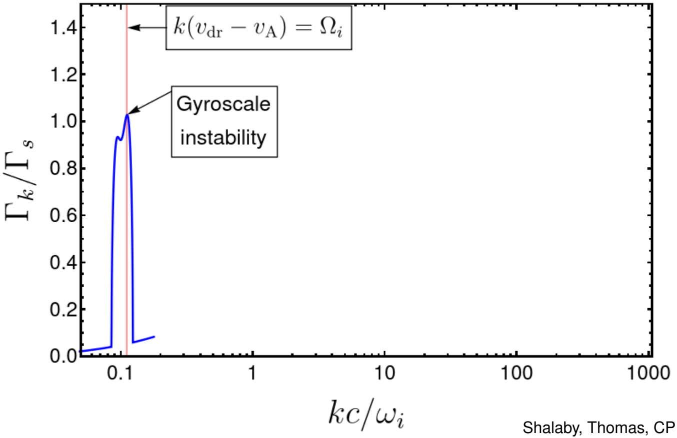

Shalaby, Thomas, CP (2021)

- gyro-resonant instability of gyrotropic CR population

CR driven instabilities – growth rates

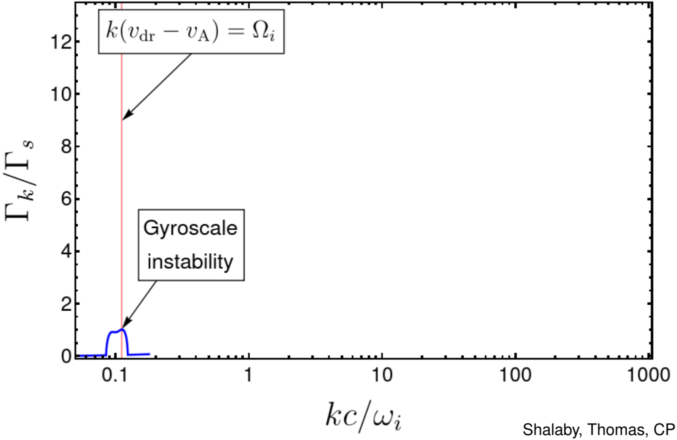

Shalaby, Thomas, CP (2021)

- gyro-resonant instability of gyrotropic CR population

CR driven instabilities – growth rates

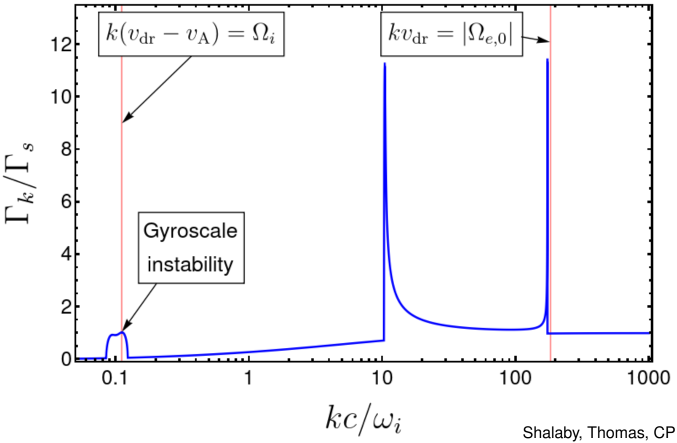

Shalaby, Thomas, CP (2021)

- **new intermediate-scale instability** of gyrotropic CR population

CR driven instabilities – growth rates

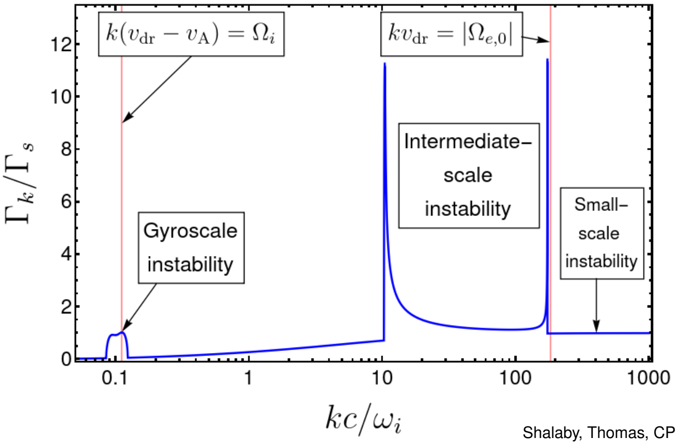

Shalaby, Thomas, CP (2021)

- **new intermediate-scale instability** of gyrotropic CR population

CR driven intermediate-scale instability

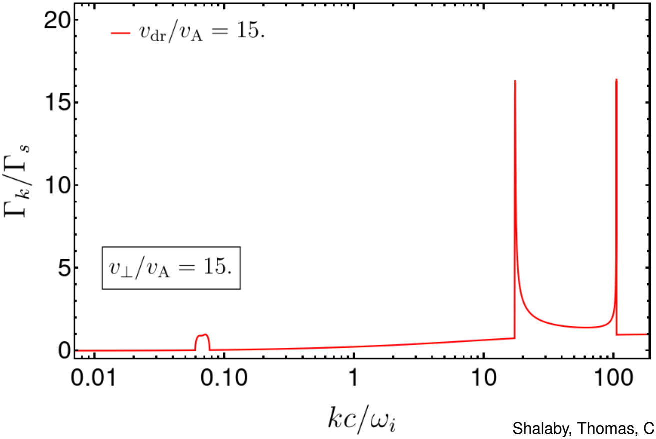

Shalaby, Thomas, CP (2021)

- low CR drift speed: two instability peaks

CR driven intermediate-scale instability

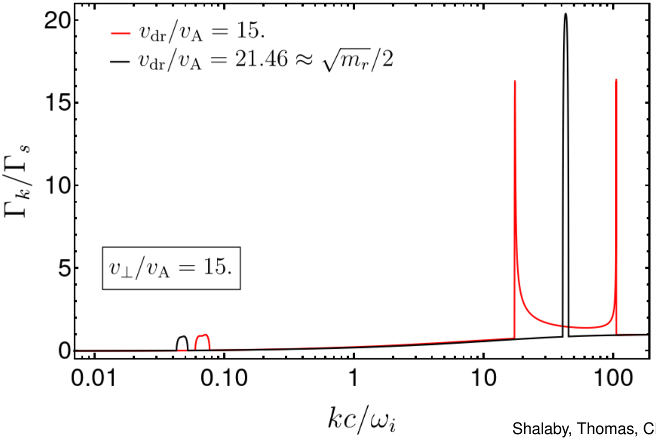

Shalaby, Thomas, CP (2021)

- for CR drift speed $v_{\rm dr} \approx \sqrt{\frac{m_{\rm i}}{m_{\rm e}}}\frac{v_{\rm A}}{2}$: two instability peaks merge

CR driven intermediate-scale instability

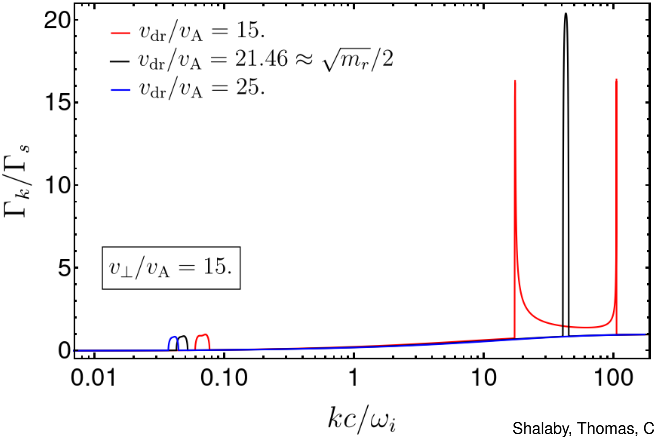

Shalaby, Thomas, CP (2021)

- for $v_{\rm dr} > \sqrt{\frac{m_{\rm i}}{m_{\rm e}}}\frac{v_{\rm A}}{2}$: intermediate-scale instability quenched

Cosmic ray driven instabilities

Growth of the intermediate-scale and the gyro-resonant instability

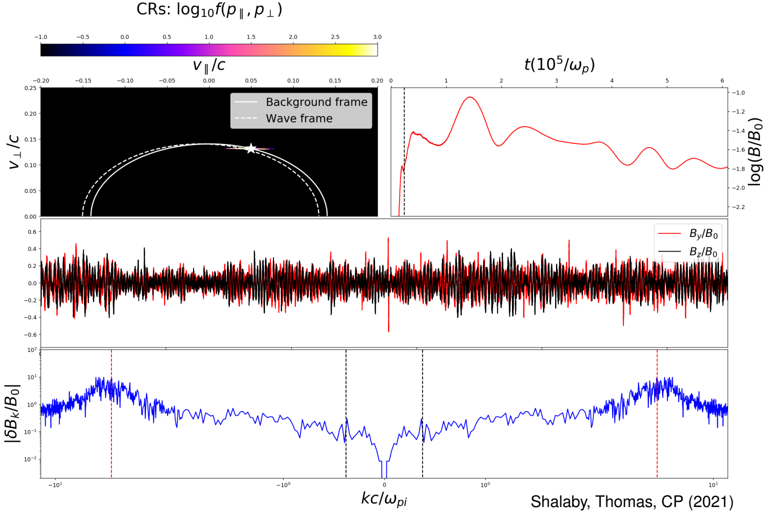

Shalaby, Thomas, CP (2021)

CR driven instabilities: magnetic field growth

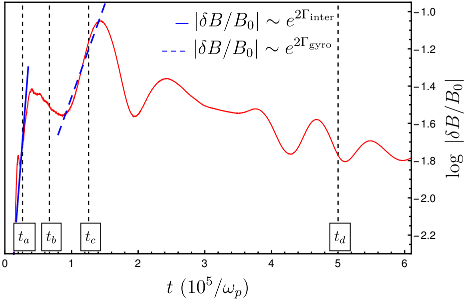

Shalaby, Thomas, CP (2021)

CR driven instabilities: magnetic field growth

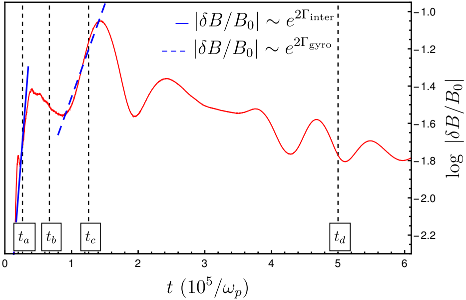

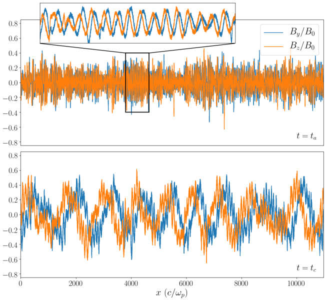

Shalaby, Thomas, CP (2021)

- $t \sim t_a$: fast magnetic field amplification at scales $< d_i$: growth of ion cyclotron waves that are comoving with CRs

CR driven instabilities: magnetic field growth

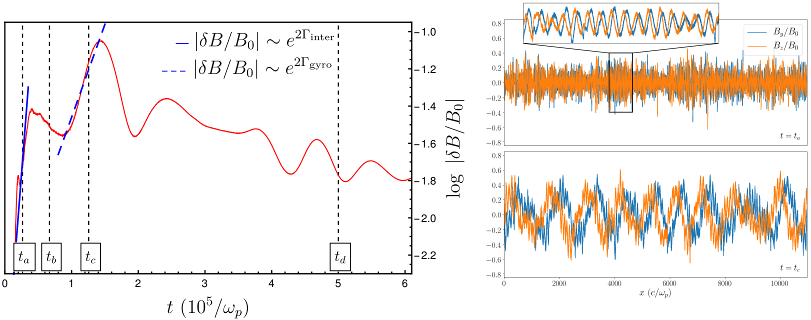

Shalaby, Thomas, CP (2021)

- $t \sim t_{\rm a}$: fast magnetic field amplification at scales $< d_{\rm i}$: growth of ion cyclotron waves that are comoving with CRs
- $t \sim t_{\rm c}$: instability starts to grow on larger, gyro-resonant scale $d_{\rm i}$: growth of resonant Alfvén waves

CR driven instabilities: momentum distribution

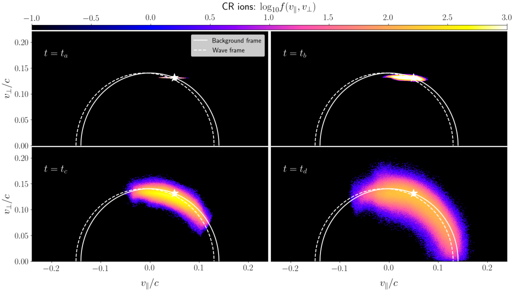

Shalaby, Thomas, CP (2021)

CR driven instabilities: momentum distribution

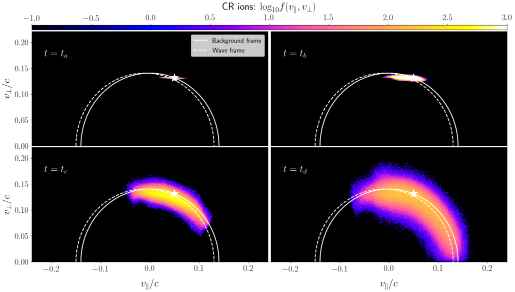

Shalaby, Thomas, CP (2021)

electromagnetic wave with $v_{\rm ph}$ interacting with particle of velocity (v_x, v_y, v_z):

$$\dot{K}_\parallel = \frac{m}{2}\frac{dv_x^2}{dt} = q v_x (v_y B_z - v_z B_y)$$

$$\dot{K}_\perp = \frac{m}{2}\frac{dv_\perp^2}{dt} = -q\left[(v_x - v_{\rm ph}) v_y B_z - (v_x - v_{\rm ph}) v_z B_y\right]$$

CR driven instabilities: momentum distribution

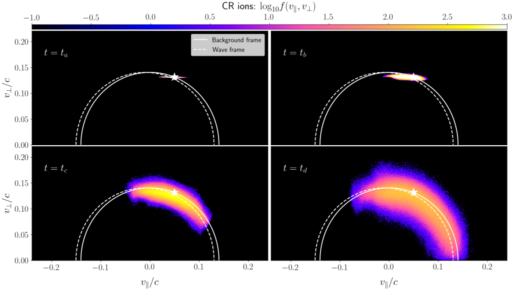

Shalaby, Thomas, CP (2021)

electromagnetic wave with $v_{\rm ph}$ interacting with particle of velocity (v_x, v_y, v_z):

$$\dot{K}_\parallel = \frac{m}{2}\frac{dv_x^2}{dt} = q v_x (v_y B_z - v_z B_y)$$

$$\dot{K}_\perp = \frac{m}{2}\frac{dv_\perp^2}{dt} = -q\left[(v_x - v_{\rm ph}) v_y B_z - (v_x - v_{\rm ph}) v_z B_y\right]$$

- $t \sim t_a$: $v_x \approx v_{\rm ph}$ $\Rightarrow$ $\dot{K}_\perp \approx 0$: parallel scattering only

CR driven instabilities: momentum distribution

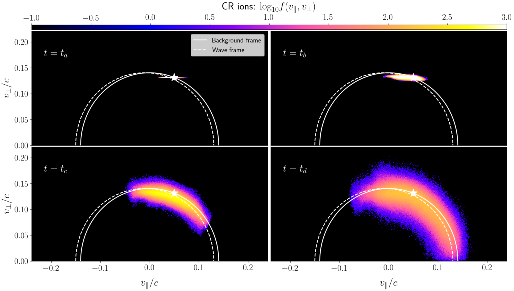

Shalaby, Thomas, CP (2021)

electromagnetic wave with v_{ph} interacting with particle of velocity (v_x, v_y, v_z):

$$\dot{K}_\parallel = \frac{m}{2}\frac{dv_x^2}{dt} = qv_x(v_yB_z - v_zB_y)$$

$$\dot{K}_\perp = \frac{m}{2}\frac{dv_\perp^2}{dt} = -q\left[(v_x - v_{\mathrm{ph}})v_yB_z - (v_x - v_{\mathrm{ph}})v_zB_y\right]$$

- $t \sim t_a$: $v_x \approx v_{\mathrm{ph}}$ $\Rightarrow$ $\dot{K}_\perp \approx 0$: parallel scattering only
- $t \sim t_c$: $v_{\mathrm{ph}} \approx 0$ $\Rightarrow$ $\dot{K}_\perp \approx -\dot{K}_\parallel$: energy-conserving scattering

AIP

Regimes of CR driven instabilities

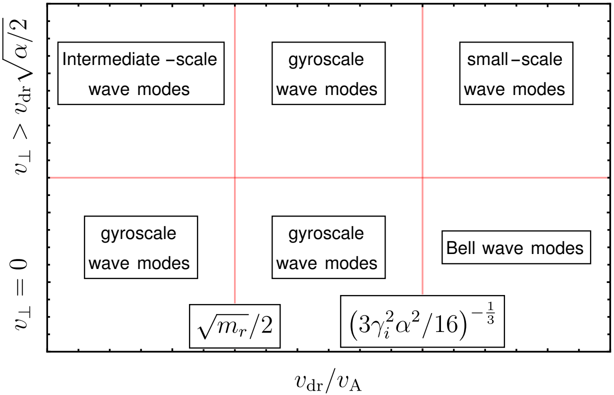

Shalaby, Thomas, CP (2021)

- where $\alpha = \frac{n_{\rm cr}}{n_{\rm i}}$ is the CR number fraction, $m_{\rm r} = \frac{m_{\rm i}}{m_{\rm e}}$ is the mass ratio, and $\gamma_{\rm i}$ is the Lorentz factor of CR ions

The intermediate-scale instability

Properties of the intermediate-scale instability:

- growth rate $\Gamma_{\mathrm{inter}} \gg \Gamma_{\mathrm{gyro}}$ and excites broad spectral support
- unstable modes are background ion-cyclotron waves in the comoving CR frame
- condition for growth: $$\frac{v_{\mathrm{dr}}}{v_{\mathrm{A}}} < \frac{1}{2}\sqrt{\frac{m_{\mathrm{i}}}{m_{\mathrm{e}}}}$$

AIP

The intermediate-scale instability

Properties of the intermediate-scale instability:

- growth rate $\Gamma_{\mathrm{inter}} \gg \Gamma_{\mathrm{gyro}}$ and excites broad spectral support
- unstable modes are background ion-cyclotron waves in the comoving CR frame
- condition for growth: $$\frac{v_{\mathrm{dr}}}{v_{\mathrm{A}}} < \frac{1}{2}\sqrt{\frac{m_{\mathrm{i}}}{m_{\mathrm{e}}}}$$

Possible implications of this new instability:

- couples CRs more tightly to background plasma and strengthens CR feedback in galaxies and galaxy clusters
- slows down CR escape from the sites of particle acceleration $\rightarrow$ brighter gamma-ray halos
- enables electron heating at shocks and injection into diffusive shock acceleration

Electron acceleration at non-relativistic shocks

electron injection problem:

- gyro-radii: $r_\mathrm{e} = \frac{m_\mathrm{e}}{m_\mathrm{i}} r_\mathrm{i} \Rightarrow$ electrons do *random walk* through the shock transition; no coherent electrostatic shock potential

Electron acceleration at non-relativistic shocks

electron injection problem:

- gyro-radii: $r_\mathrm{e} = \frac{m_\mathrm{e}}{m_\mathrm{i}}\, r_\mathrm{i} \Rightarrow$ electrons do *random walk* through the shock transition; no coherent electrostatic shock potential
- intermediate-scale instability provides large-amplitude magnetic fluctuations at sub ion-gyroscale

Electron acceleration at non-relativistic shocks

electron injection problem:

- gyro-radii: $r_\mathrm{e} = \frac{m_\mathrm{e}}{m_\mathrm{i}} r_\mathrm{i} \Rightarrow$ electrons do *random walk* through the shock transition; no coherent electrostatic shock potential
- intermediate-scale instability provides large-amplitude magnetic fluctuations at sub ion-gyroscale $\Rightarrow$ ***a solution? PIC simulations***

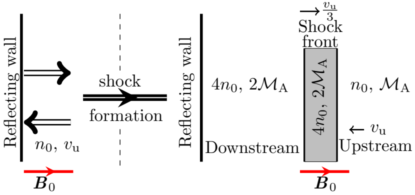

Shalaby, Lemmerz, Thomas, CP (2022):
quasi-parallel, non-relativistic shock with PIC code SHARP

Electron acceleration at non-relativistic shocks

electron injection problem:

- gyro-radii: $r_\mathrm{e} = \frac{m_\mathrm{e}}{m_\mathrm{i}} r_\mathrm{i} \Rightarrow$ electrons do *random walk* through the shock transition; no coherent electrostatic shock potential
- intermediate-scale instability provides large-amplitude magnetic fluctuations at sub ion-gyroscale $\Rightarrow$ ***a solution? PIC simulations***

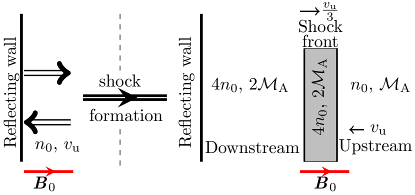

Shalaby, Lemmerz, Thomas, CP (2022):
quasi-parallel, non-relativistic shock with PIC code SHARP

Table 1
Parameters of our electron-ion parallel shock simulations

Name	v_u/c[a]	$\mathcal{M}_\mathrm{A}$[b]	$\mathcal{M}_s$[c]	m_i/m_e	Condition[d]
Ma5Mr1836	-0.1	5.3	365	1836	✓
Ma5Mr100	-0.1	5.3	365	100	×
Ma21Mr1836	-0.1	21.3	365	1836	×

condition in front/downstream:

$$\mathcal{M}_\mathrm{A} \lesssim \frac{1}{4}\sqrt{\frac{m_\mathrm{i}}{m_\mathrm{e}}}$$

Particle acceleration at a non-relativistic shock

The intermediate-scale and the gyro-resonant instabilities mediate particle scattering

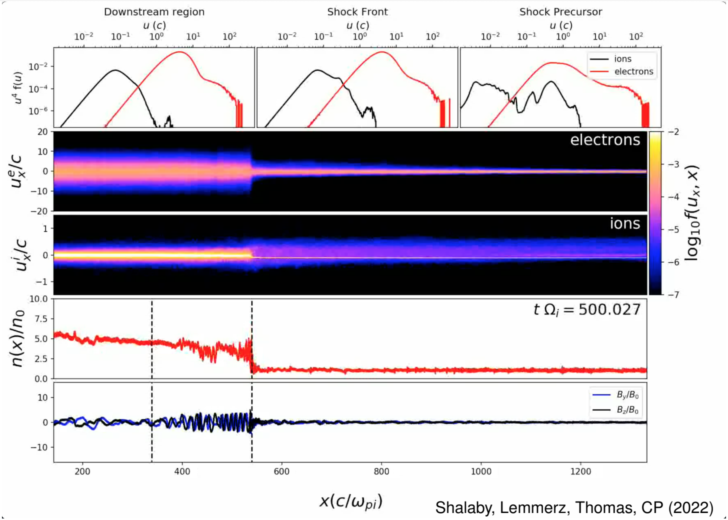

Shalaby, Lemmerz, Thomas, CP (2022)

Shock acceleration: intermediate-scale instability

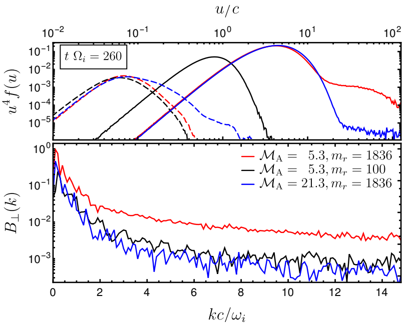

Shalaby, Lemmerz, Thomas, CP (2022)

- only red simulation, which grows intermediate-scale instability, accelerates electrons
- red simulation amplifies the magnetic field ten times more

Shock acceleration efficiency: K_{ei}

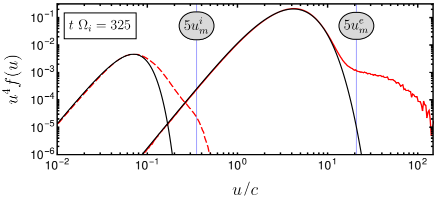

- rest-frame momentum distribution of ions and electrons
- analytical Maxwell-Jüttner distribution normalized to u_m, for which $u^4 f(u)$ is maximum

Shock acceleration efficiency: K_{ei}

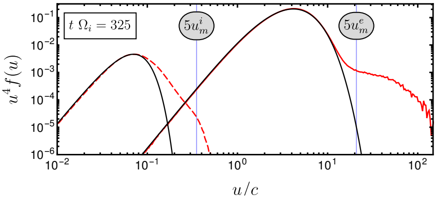

- rest-frame momentum distribution of ions and electrons
- analytical Maxwell-Jüttner distribution normalized to u_{m}, for which $u^4 f(u)$ is maximum
- non-thermal electron-to-ion energy:

$$K_{\mathrm{ei}} = \frac{E_{\mathrm{e}}(u > 5u_{\mathrm{m}}^{\mathrm{e}})}{E_{\mathrm{i}}(u > 5u_{\mathrm{m}}^{\mathrm{i}})}$$

Shock acceleration efficiency: $K_{\rm ei}$

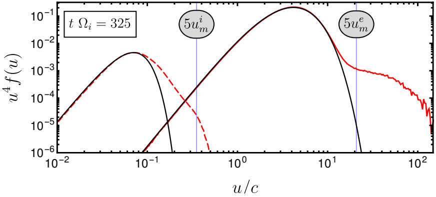

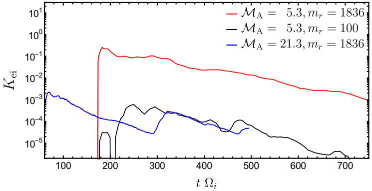

Shalaby, Lemmerz, Thomas, CP (2022)

- rest-frame momentum distribution of ions and electrons
- analytical Maxwell-Jüttner distribution normalized to $u_{\rm m}$, for which $u^4 f(u)$ is maximum
- non-thermal electron-to-ion energy:

$$K_{\rm ei} = \frac{E_{\rm e}(u > 5u^{\rm e}_{\rm m})}{E_{\rm i}(u > 5u^{\rm i}_{\rm m})}$$

- downstream evolution of $K_{\rm ei}$ (non-thermal ion distribution still growing)
- $\mathcal{M}_{\rm s}$ and $v_{\rm sh}$ identical for all runs, only $\mathcal{M}_{\rm A}$ differs

Shock acceleration efficiency: K_{ei}

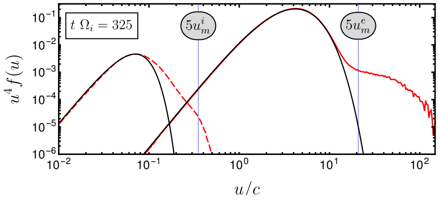

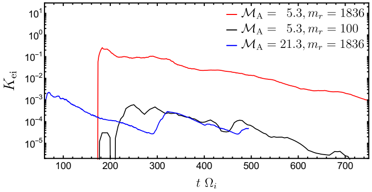

Shalaby, Lemmerz, Thomas, CP (2022)

- rest-frame momentum distribution of ions and electrons
- analytical Maxwell-Jüttner distribution normalized to u_m, for which $u^4 f(u)$ is maximum
- non-thermal electron-to-ion energy:

$$K_{\mathrm{ei}} = \frac{E_\mathrm{e}(u > 5u_\mathrm{m}^\mathrm{e})}{E_\mathrm{i}(u > 5u_\mathrm{m}^\mathrm{i})}$$

- downstream evolution of K_{ei} (non-thermal ion distribution still growing)
- $\mathcal{M}_\mathrm{s}$ and v_sh identical for all runs, only $\mathcal{M}_\mathrm{A}$ differs
- ***presence of intermediate-scale instability increases K_{ei} by more than 100!***

AIP

Shock dissipation: electron and ion temperatures

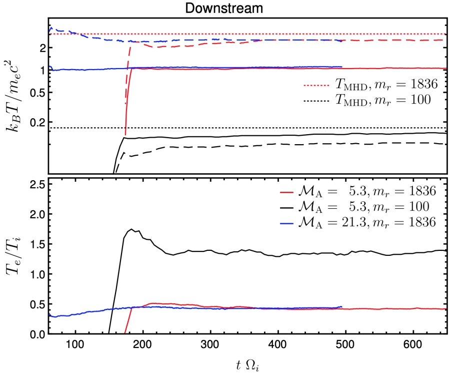

Shalaby, Lemmerz, Thomas, CP (2022)

- time evolution of downstream T_i (dashed) and T_e (solid)

Shock dissipation: electron and ion temperatures

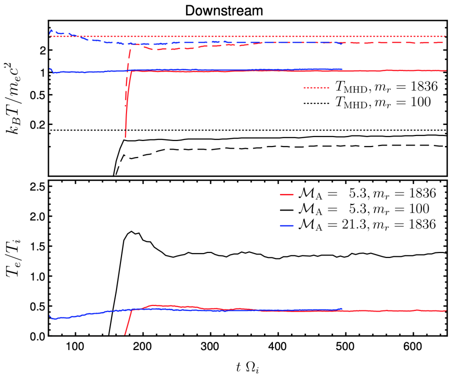

Shalaby, Lemmerz, Thomas, CP (2022)

- time evolution of downstream $T_{\rm i}$ (dashed) and $T_{\rm e}$ (solid)

- runs with $m_{\rm i}/m_{\rm e} = 1836$ have different efficiencies $K_{\rm ei}$ but same temperatures

Shock dissipation: electron and ion temperatures

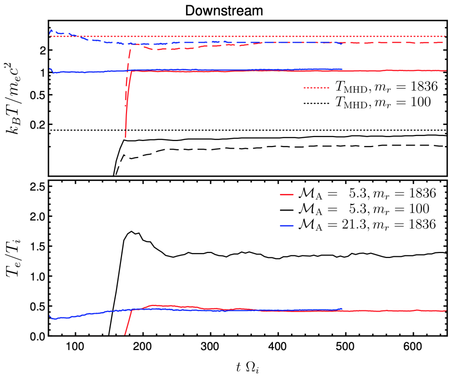

Shalaby, Lemmerz, Thomas, CP (2022)

- time evolution of downstream $T_{\rm i}$ (dashed) and $T_{\rm e}$ (solid)

- runs with $m_{\rm i}/m_{\rm e} = 1836$ have different efficiencies $K_{\rm ei}$ but same temperatures
- $T_{\rm i}$ equilibrates to MHD value (deviations due to CR and magnetic energies)
- $T_{\rm e} \approx 0.4\, T_{\rm i}$ (1D vs. 3D or missing instabilities?)

AIP

Shock dissipation: electron and ion temperatures

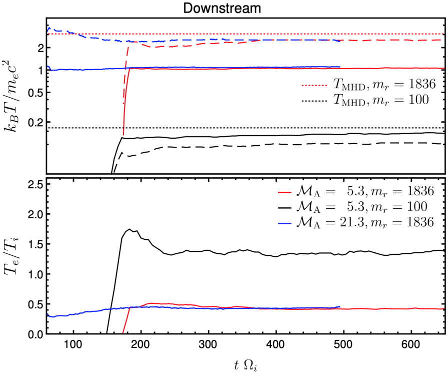

Shalaby, Lemmerz, Thomas, CP (2022)

- time evolution of downstream $T_{\rm i}$ (dashed) and $T_{\rm e}$ (solid)

- runs with $m_{\rm i}/m_{\rm e} = 1836$ have different efficiencies $K_{\rm ei}$ but same temperatures
- $T_{\rm i}$ equilibrates to MHD value (deviations due to CR and magnetic energies)
- $T_{\rm e} \approx 0.4\,T_{\rm i}$ (1D vs. 3D or missing instabilities?)
- true $m_{\rm i}/m_{\rm e}$ required for correct heating physics

Electron acceleration at non-relativistic shocks

Intermediate-scale instability at shocks:

- provides efficient pre-acceleration that scatters and accelerates electrons on scales much shorter than the ion gyro radius
- instability drives comoving ion-cyclotron waves (with the upstream plasma) at the shock front
- condition for growth: $$\frac{v_{\mathrm{sh}}}{v_{\mathrm{A},0}} < \frac{1}{4}\sqrt{\frac{m_{\mathrm{i}}}{m_{\mathrm{e}}}}, \quad \text{for} \quad n = 4n_0$$

AIP

Electron acceleration at non-relativistic shocks

Intermediate-scale instability at shocks:

- provides efficient pre-acceleration that scatters and accelerates electrons on scales much shorter than the ion gyro radius
- instability drives comoving ion-cyclotron waves (with the upstream plasma) at the shock front
- condition for growth: $\frac{v_{\mathrm{sh}}}{v_{\mathrm{A},0}} < \frac{1}{4}\sqrt{\frac{m_{\mathrm{i}}}{m_{\mathrm{e}}}}, \quad \text{for} \quad n = 4n_0$

Electron shock acceleration and heating:

- intermediate-scale instability increases electron acceleration efficiency (by factor > 100)
- ion thermalization in line with MHD (accounting for E_B and E_{CR}), but $T_{\mathrm{e}} \approx 0.4\,T_{\mathrm{i}}$ remains open question
- reduced $m_{\mathrm{i}}/m_{\mathrm{e}}$ suppresses intermediate instability, precludes electron acceleration, results in erroneous electron and ion heating

Global MHD simulations of SNRs with CR physics

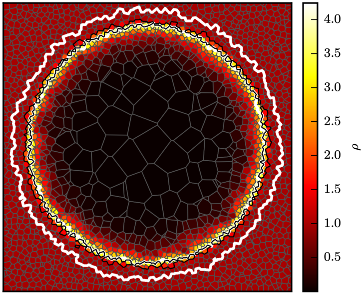

Mach number finder with CRs

CP+ (2017)

- detect and characterize shocks and jump conditions on the fly

Global MHD simulations of SNRs with CR physics

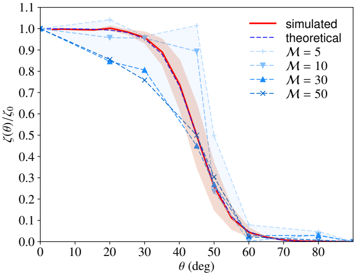

obliquity-dep. acceleration efficiency

Pais, CP+ (2018) based on
hybrid PIC sim.'s by Caprioli & Spitkovsky (2015)

- detect and characterize shocks and jump conditions on the fly
- measure Mach number $\mathcal{M}$ and magnetic obliquity θ_B

AIP

Global MHD simulations of SNRs with CR physics

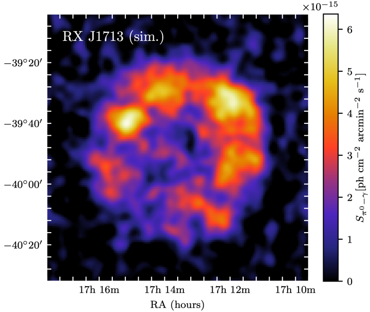

simulated TeV gamma-ray map

Pais & CP (2020)

- detect and characterize shocks and jump conditions on the fly
- measure Mach number $\mathcal{M}$ and magnetic obliquity θ_B
- inject and transport CR protons $\Rightarrow$ dynamical back reaction on gas flow, hadronic emission

Global MHD simulations of SNRs with CR physics

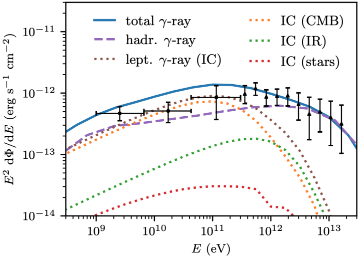

simulated gamma-ray spectrum

Winner, CP+ (2019, 2020)

- detect and characterize shocks and jump conditions on the fly
- measure Mach number $\mathcal{M}$ and magnetic obliquity θ_B
- inject and transport CR protons $\Rightarrow$ dynamical back reaction on gas flow, hadronic emission
- inject and transport CR electrons
- calculate non-thermal radio, X-ray, γ-ray emission

Hadronic TeV γ rays: SN 1006

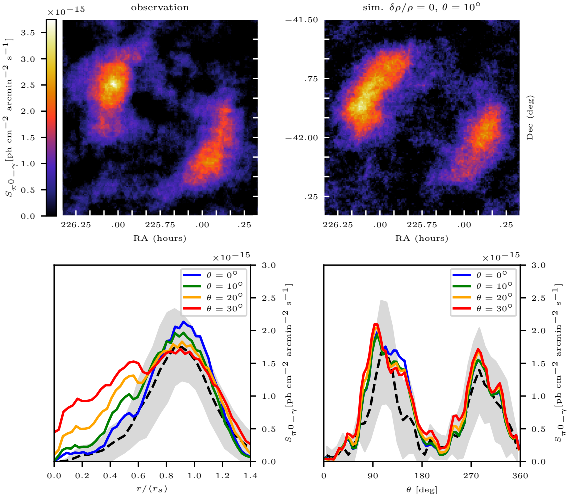

Pais & CP (2020)

Hadronic TeV γ rays: SN 1006

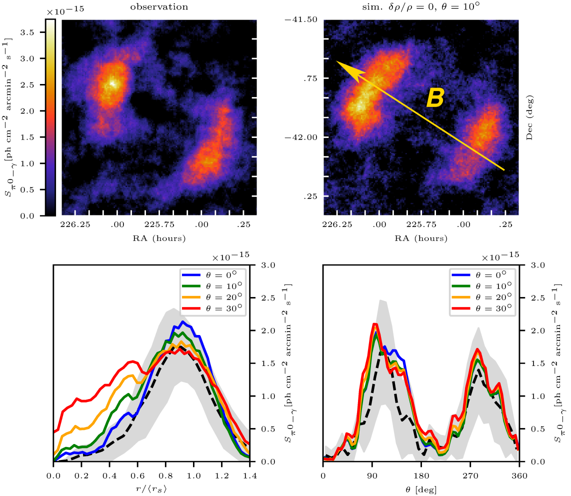

Pais & CP (2020)

Hadronic TeV γ rays: Vela Jr. and RXJ 1713

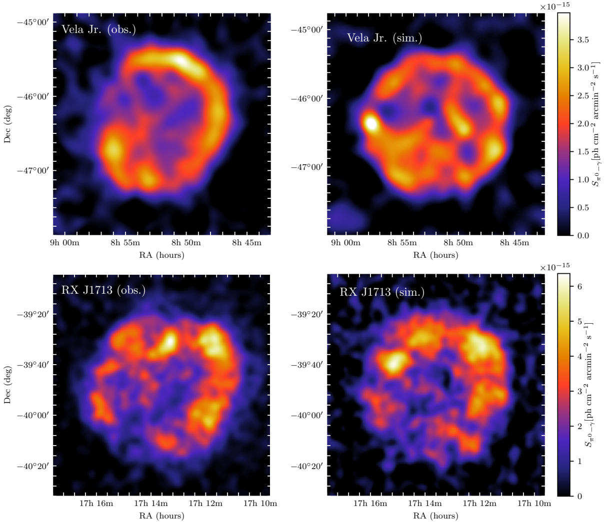

Pais & CP (2020)

TeV γ rays from shell-type supernova remnants

Varying magnetic coherence scale in simulations of SN 1006 and Vela Junior

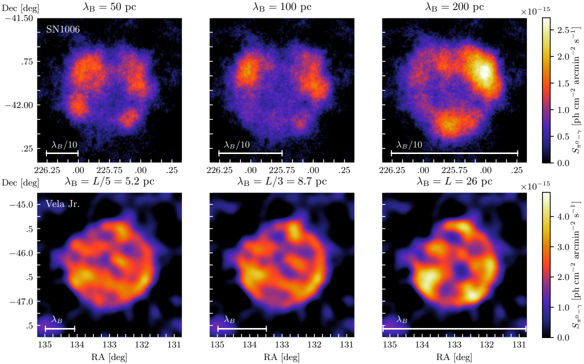

TeV γ rays from shell-type supernova remnants

Varying magnetic coherence scale in simulations of SN 1006 and Vela Junior

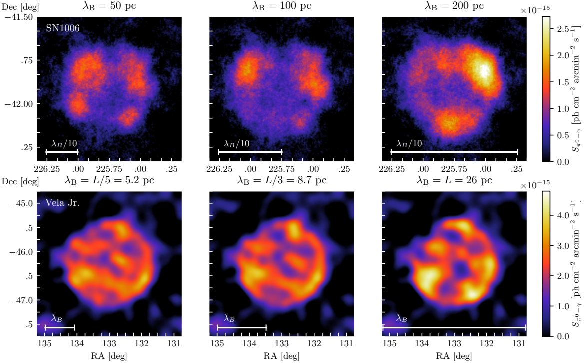

Pais, CP+ (2020)

$\Rightarrow$ Correlation structure of patchy TeV γ-rays constrains magnetic coherence scale in ISM:

SN 1006: $\lambda_B > 200^{+80}_{-10}$ pc   Vela Junior: $\lambda_B = 13^{+13}_{-4.3}$ pc

CREST - Cosmic Ray Electron Spectra evolved in Time

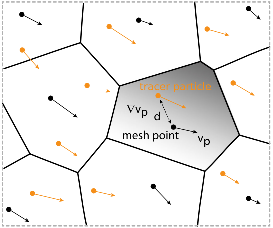

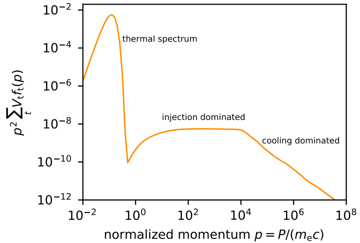

CREST code (Winner, CP+ 2019)

- post-processing MHD simulations
- on Lagrangian particles
  - adiabatic processes
  - Coulomb and radiative losses
  - Fermi-I (re-)acceleration
  - Fermi-II reacceleration
  - secondary electrons

Link to observations

- radio synchrotron
- inverse Compton (IC) γ-ray

Sedov–Taylor blast wave: spectral evolution

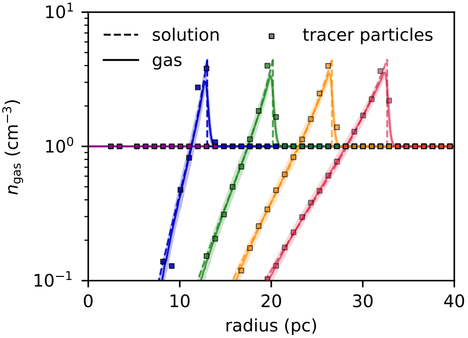

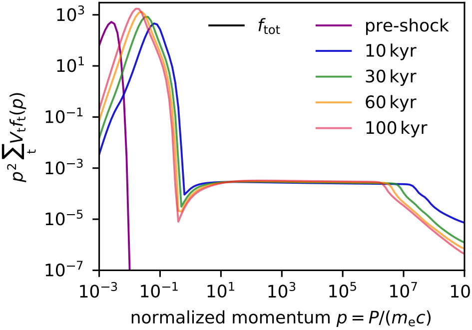

Winner, CP+ (2019)

$E_0 = 10^{51}\,\mathrm{erg},\ n_{\mathrm{gas}} = 1\,\mathrm{cm}^{-3},\ T_0 = 10^4\,\mathrm{K},\ B = 1\,\mu\mathrm{G}$

SN 1006: CR electron acceleration models

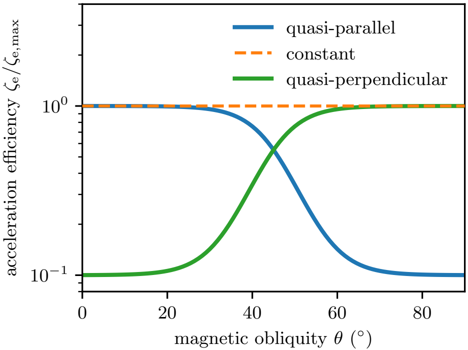

Winner, CP+ (2020)

- different obliquity dependent electron acceleration efficiencies:
  1. preferred quasi-perpendicular acceleration (previous PIC)
  2. constant acceleration efficiency (a straw man's model)
  3. preferred quasi-parallel acceleration (like CR protons)

CR electron acceleration: quasi-perpendicular shocks

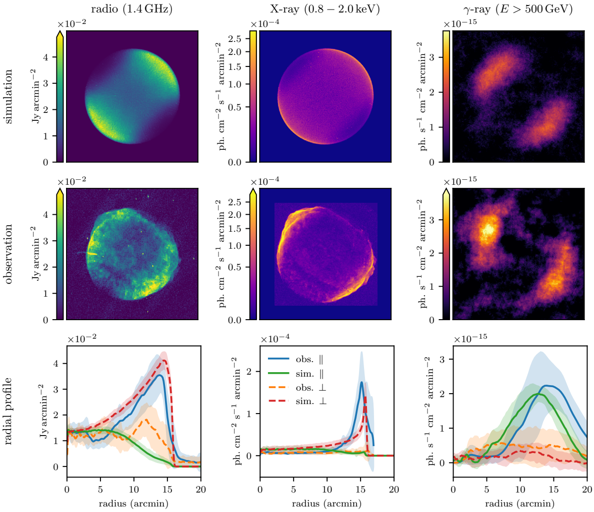

Winner, CP+ (2020)

CR electron acceleration: constant efficiency

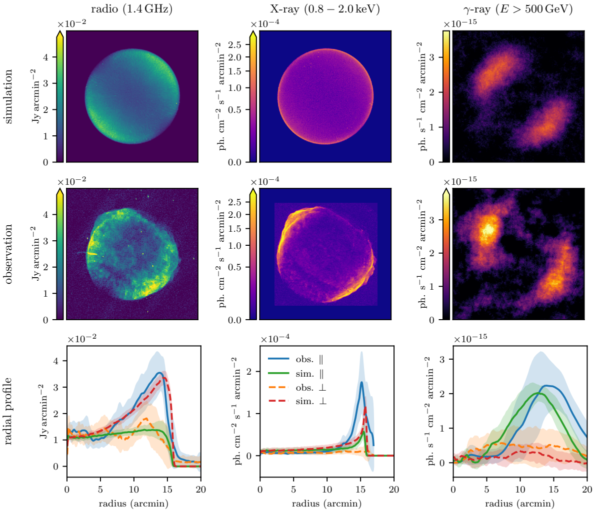

Winner, CP+ (2020)

CR electron acceleration: quasi-parallel shocks

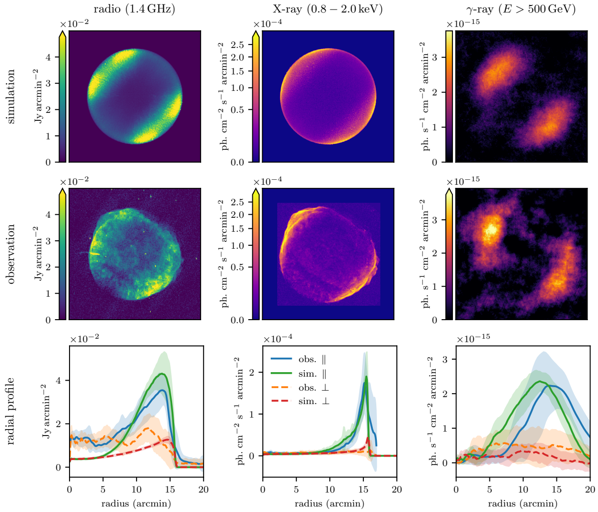

Winner, CP+ (2020)

SN 1006: multi-frequency spectrum

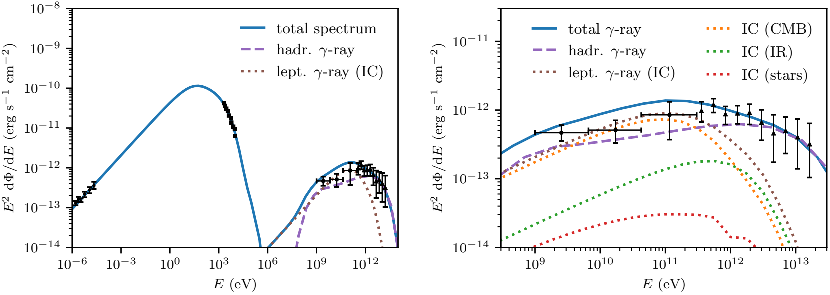

Winner, CP+ (2020)

- quasi-parallel acceleration model fits multi-frequency spectrum

SN 1006: multi-frequency spectrum

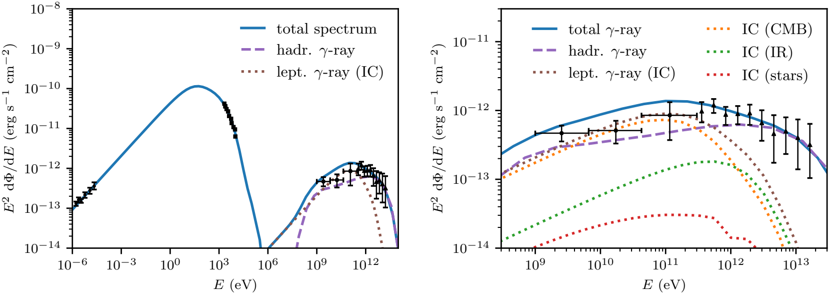

Winner, CP+ (2020)

- quasi-parallel acceleration model fits multi-frequency spectrum
- GeV regime: leptonic inverse Compton dominates
- TeV regime: hadronic pion decay

Conclusions for CR hydrodynamics at SNRs

CR hydrodynamics with kinetic plasma physics:

- Shock finder enables CR acceleration in MHD simulations
- CR proton transport in MHD enables dynamic backreaction
- CR electron spectral transport (CREST): multi-frequency spectra and emission maps

Conclusions for CR hydrodynamics at SNRs

CR hydrodynamics with kinetic plasma physics:

- Shock finder enables CR acceleration in MHD simulations
- CR proton transport in MHD enables dynamic backreaction
- CR electron spectral transport (CREST): multi-frequency spectra and emission maps

CR acceleration constraints by MHD models:

- TeV shell-type SNRs probe magnetic coherence scale in ISM
- hybrid-PIC simulations of p^+ acceleration agree with global SNR simulations
- global SNR simulations imply preferred quasi-parallel e^- acceleration: new intermediate instability enables e^- (pre-)acceleration

PICOGAL: From Plasma KInetics to COsmological GALaxy Formation

This project has received funding from the European Research Counsil (ERC) under the European Union's Horizon 2020 research and innovation program (grant agreement No PICOGAL–101019746).

Literature for the talk – 1

Cosmic ray driven instabilities:

- Shalaby, Thomas, Pfrommer, *A new cosmic ray-driven instability,* 2021, ApJ, 908, 206.
- Shalaby, Lemmerz, Thomas, Pfrommer, *The mechanism of efficient electron acceleration at parallel non-relativistic shocks,* 2022, ApJ, 932, 86.

Cosmic ray hydrodynamics and shock acceleration:

- Pfrommer, Pakmor, Schaal, Simpson, Springel, *Simulating cosmic ray physics on a moving mesh* 2017, MNRAS, 465, 4500.

Literature for the talk – 2

Cosmic ray electron spectra in MHD:

- Winner, Pfrommer, Girichidis, Pakmor, *Evolution of cosmic ray electron spectra in magnetohydrodynamical simulations,* 2019, MNRAS, 488, 2235.
- Winner, Pfrommer, Girichidis, Werhahn, Pais, *Evolution and observational signatures of the cosmic ray electron spectrum in SN 1006,* 2020, MNRAS, 499, 2785.

Cosmic ray proton acceleration at SNRs:

- Pais, Pfrommer, Ehlert, Pakmor, *The effect of cosmic-ray acceleration on supernova blast wave dynamics,* 2018, MNRAS, 478, 5278.
- Pais, Pfrommer, Ehlert, Werhahn, Winner, *Constraining the coherence scale of the interstellar magnetic field using TeV gamma-ray observations of supernova remnants,* 2020, MNRAS, 496, 2448.
- Pais, Pfrommer, *Simulating TeV gamma-ray morphologies of shell-type supernova remnants,* 2020, MNRAS, 498, 5557.